A GAIN-SCHEDULING APPROACH FOR AIRSHIP PATH-TRACKING

Alexandra Moutinho

IDMEC - IST

Instituto Superior Técnico, Av. Rovisco Pais, 1047-001 Lisbon, Portugal

José Raul Azinheira

IDMEC - IST

Instituto Superior Técnico, Av. Rovisco Pais, 1047-001 Lisbon, Portugal

Keywords: UAV, gain-scheduling, path-tracking, optimal control, airship.

Abstract: In this paper a gain scheduled optimal controller is designed to solve the path-tracking problem of an airship. The control law is obtained from a coupled linear model of the airship that allows to control the longitudinal and lateral motions simultaneously. Due to the importance of taking into account wind effects, which are rather important due to the airship large volume, the wind is included in the kinematics, and the dynamics is expressed as function of the air velocity. Two examples are presented with the inclusion of wind, one considering a constant wind input and the other considering in addition a 3D turbulent gust, demonstrating the effectiveness of this single controller tracking a reference path over the entire flight envelope.

1 INTRODUCTION

The range of civilian and military applications of Unmanned Aerial Vehicles (UAV's) is driving the growth of the rapidly changing market for UAVs globally. The list of applications and opportunities in this domain is already large and is continually growing. Among these are inspection oriented applications that cover different areas such as mineral and archaeologic prospecting, land use surveys in rural and urban regions, inspection of man-made structures such as pipelines, power transmission lines, dams and roads.

Most of the applications cited above have profiles that require maneuverable low altitude, low speed airborne data gathering platforms. The vehicle should also be able to hover above an observation target, present extended airborne capabilities for long duration studies, take-off and land vertically without the need of runway infrastructures, have a large payload to weight ratio, among other requisites. For this scenario, lighter-than-air (LTA) vehicles, like airships, are often better suited than balloons, airplanes and helicopters (Elfes et al., 1998), mainly because: they derive the largest part of their lift from aerostatic, rather than aerodynamic forces; they are safer and, in case of failure, present a graceful degradation; they are intrinsically of higher stability than other platforms.

For all its advantages, airships are being chosen as platform to a variety of applications. Some examples are demining[1], fire detection (Merino et al., 2005), emergency management (Rao et al., 2005), target search (Xia and Corbett, 2005) and even exploration of planetary bodies (Elfes et al., 2003).

In some cases, the airship is remotely maneuvered, but a wider range of applications is achievable with unmanned autonomous airships, which requires an effective control of the robot behavior. Like other aerial vehicles, the airship dynamics is highly nonlinear. It mostly varies with the relative airspeed, which influences both acting forces as well as actuators authority. In flight control design, it is an established practice to base the controller design in a linear description of the system, obtained assuming the motion of the aerial vehicle is constrained to small perturbations about a trimmed equilibrium flight condition (Stevens and Lewis, 1992). For instance, Hygounenc and Souères consider linear decoupled models for the longitudinal and lateral motions. The vertical movement is regulated using a Lyapunov based approach, while the horizontal path-following problem is independently solved with a PI controller (Hygounenc and Souères, 2003). Xia and Corbett apply the sliding mode technique to the linear decoupled systems in order to obtain a cooperative control system for two blimps (Xia and Corbett, 2005). Complementing the linear model of the airship with the vector of visual signals, Silveira *et al.* report a line following visual servo control

---

[1]www.mineseeker.com

scheme with a PID structure (Silveira et al., 2003).

Although using different control methodologies, the above references all implicitly use the gain scheduling approach (Åström and Wittenmark, 1989; Khalil, 2000a), the prevailing flight control design methodology nowadays (Rugh and Shamma, 2000). As mentioned, the linear model of the system is an approximation only valid for small perturbations around an equilibrium condition, which leads to the necessity of repeating the linearization process for several trim points over the desired operation range.

In this paper a gain scheduled optimal controller is designed to solve the path-tracking problem for the airship of the Aurora (Autonomous Unmanned Remote mOnitoring Robotic Airship) project (de Paiva et al., 2006). The control law is obtained from a coupled linear model of the airship that allows to control the longitudinal and lateral motions simultaneously. Due to the importance of taking into account wind effects, which are rather important due to the airship large volume, the wind is included in the kinematics, and the dynamics is expressed as function of the air velocity. The designed controller has been tested exhaustively in simulation environment prior to real implementation, and effective results have been obtained covering the entire flight envelope with the single controller. We present here two cases concerning the same reference tracking: a nominal case and a case considering realistic wind disturbances, which the airship platform is supposed to face during its normal operation.

In this article we start by describing the Aurora airship platform, followed by the definition of the model used in the control design (§ 2). In § 4 we propose an optimal gain scheduled control, applied to the path-tracking problem in § 3. So as to illustrate the valuable results obtained, in § 5 we show examples of the proposed control acting over the entire flight envelope in the presence of wind disturbances. Finally, conclusions are summarized in § 6.

2 AIRSHIP DESCRIPTION

2.1 Airship Platform

In this section we briefly describe the airship platform of the Aurora project (de Paiva et al., 2006).

The LTA robotic prototype has been built as an evolution of the Airspeed Airships' AS800. It is a non-rigid airship with $10.5m$ long, $3.0m$ diameter, and $34m^3$ of volume, whose payload capacity is approximately $10kg$ and maximum speed is around $50km/h$ (see fig. 1). As main control actuators, the airship has: *i)* four deflection surfaces at the tail in the '$\times$' configuration; *ii)* the thrust provided by two propellers

driven by two-stroke engines; *iii)* the vectoring of this propulsion group.

Figure 1: The Aurora airship.

The airship system state variables are measured by a GPS with differential correction, an inertial measurement unit and a wind sensor.

2.2 Airship Model

Consider an underactuated airship modeled as a rigid body subject to forces and torques. Let $\{i\}$ represent the inertial frame (which, for simplicity, is considered coincident with the geographical north-east-down (NED) frame), $\{l\}$ be the body-fixed coordinate frame whose origin is located in the airship center of volume, and $\mathbf{S}(\mathbf{\Phi}) \in SO(3) := \{\mathbf{S} \in \mathbb{R}^{3\times3} : \mathbf{SS}' = \mathbf{I}, \det(\mathbf{S}) = +1\}$ is the rotation matrix from $\{i\}$ to $\{l\}$ frame, and where $\mathbf{\Phi} \in \mathbb{R}^{3\times1}$ is the attitude of $\{l\}$ in relation to $\{i\}$ expressed as the Euler angles roll ϕ, pitch θ and yaw ψ.

The airship dynamic equations of motion (Azinheira et al., 2002) may be condensed in the form

$$\mathbf{M\dot{V}} = -\mathbf{\Omega}_6\mathbf{MV} + \mathbf{ESg} + \mathbf{F}_a + \mathbf{f}(\mathbf{U}_a, V_t) \quad (1)$$

$$\mathbf{\dot{P}} = \mathbf{JV} \quad (2)$$

where $\mathbf{V} = [\mathbf{v}', \boldsymbol{\omega}']' \in \mathbb{R}^{6\times1}$ includes the airship linear and angular velocities relative to $\{i\}$ expressed in $\{l\}$, $\mathbf{P} = [\mathbf{p}', \mathbf{\Phi}']' \in \mathbb{R}^{6\times1}$ contains the airship cartesian and angular positions expressed in the $\{i\}$ frame, $\mathbf{J} = \text{diag}\{\mathbf{S}', \mathbf{R}\} \in \mathbb{R}^{6\times6}$, $\mathbf{R} = \mathbf{R}(\mathbf{\Phi}) \in \mathbb{R}^{3\times3}$ is a coefficient matrix, and $\mathbf{M} \in \mathbb{R}^{6\times6}$ is the symmetric inertia matrix. $\mathbf{\Omega}_6 = \text{diag}\{\mathbf{\Omega}(\boldsymbol{\omega}), \mathbf{\Omega}(\boldsymbol{\omega})\} \in \mathbb{R}^{6\times6}$, $\mathbf{\Omega}(\boldsymbol{\omega}) \in \mathbb{R}^{3\times3}$ is the skew-symmetric matrix equivalent to the cross-product $\boldsymbol{\omega}\times$, $\mathbf{E} \in \mathbb{R}^{6\times3}$ is the gravity matrix input, and $\mathbf{g} \in \mathbb{R}^{3\times1}$ represents the gravity acceleration in the $\{i\}$ frame. $\mathbf{F}_a \in \mathbb{R}^{6\times1}$ stands for the aerodynamic forces and moments.

The input forces and torques $\mathbf{f}(\mathbf{U}_a, V_t) \in \mathbb{R}^{6\times1}$ are a nonlinear function of the airship airspeed V_t and of the actuators input $\mathbf{U}_a \in \mathbb{R}^{6\times1}$, which includes the elevator δ_e, the total left and right engines thrust X_T, the engines vectoring angle δ_v, and the rudder δ_r (see figure 2).
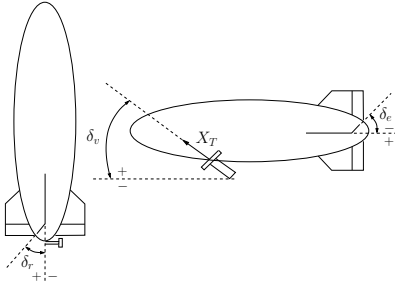
Figure 2: Airship actuators.

2.2.1 Inclusion of Wind

We assume that the inertial wind velocity vector $\dot{\mathbf{p}}_w = \mathbf{S}'\mathbf{v}_w$ is constant over a region much larger than the size of the airship. This means we do not consider wind shearing effects and torques exerted on the airship ($\boldsymbol{\omega}_w = 0$).

The velocity of the airship center of volume with respect to the air represented in the $\{l\}$ frame is given by

$$\mathbf{v}_a = \mathbf{v} - \mathbf{v}_w \qquad (3)$$

In order to include the wind influence in the airship equations of motion, the wind components must be supplied as inputs. Then $\mathbf{v}_a$, rather than $\mathbf{v}$, must be used in the calculation of the aerodynamic forces and moments. The airship dynamics and kinematics can then be rewritten as

$$\dot{\mathbf{V}}_a = \mathbf{M}^{-1}\left[-\boldsymbol{\Omega}_6\mathbf{M}\mathbf{V}_a + \mathbf{ESg} + \mathbf{F}_a + \mathbf{f}(\mathbf{U}_a)\right] \qquad (4)$$

$$\dot{\mathbf{P}} = \mathbf{J}\mathbf{V}_a + \mathbf{S}'\mathbf{V}_w \qquad (5)$$

with $\mathbf{V}_a = [\mathbf{v}'_a, \boldsymbol{\omega}']'$ and $\mathbf{V}_w = [\mathbf{v}'_w, 0]'$.

As mentioned before, the wind must be provided as input to equations (4) and (5). Since the wind is not directly measurable, we will need to compute an estimate. Knowing that

$$\mathbf{v}_a = \begin{bmatrix} V_t \cos(\alpha)\cos(\beta) \\ V_t \sin(\beta) \\ V_t \sin(\alpha)\cos(\beta) \end{bmatrix} \qquad (6)$$

where the airspeed V_t, the angle of attack α and the sideslip angle β are measurable quantities, we can compute the wind velocity vector $\mathbf{v}_w$ using equation (3).

2.2.2 Linear Model

The complexity of the nonlinear dynamic equations justifies the search for a linear simplified version, also necessary if to use the gain-scheduling approach.

The linearization of the dynamic equations (4)-(5) is made for trimmed conditions around equilibrium, which is commonly an horizontal straight flight, without wind incidence.

Considering only the dynamic or perturbed part, and for the conditions stated, the motion equations are written for a perturbation vector $\mathbf{x}$ of the states around the equilibrium value $\mathbf{X}_o$, and the perturbed input $\mathbf{u}$ around the trimmed value $\mathbf{U}_o$, resulting in the matricial dynamic equation:

$$\dot{\mathbf{x}} = \mathbf{A}\mathbf{x} + \mathbf{B}\mathbf{u} \qquad (7)$$

in the absence of disturbances (deterministic case).

The linearized model (7), i.e., the dynamic and input matrices $\mathbf{A}$ and $\mathbf{B}$, depend on the trim point chosen for the linearization, and in particular of the chosen airspeed V_{t_o} (we consider here low altitude flight, where the altitude variation is insufficient to significantly change the envelope pressure). The existence of a constant wind component is also to be considered.

In flight control, and as a result of the application of the small perturbations theory, two independent (decoupled) linear models are usually obtained, corresponding to the lateral and longitudinal motions (Stevens and Lewis, 1992). Here, we chose to work with a single linear model, which allows us to design a single controller for the lateral and longitudinal movements.

Considering that all variables now correspond to the perturbation term, the state and input vectors of the dynamics equation (7) are $\mathbf{x} = [\mathbf{v}'_a, \boldsymbol{\omega}', \mathbf{p}', \boldsymbol{\Phi}']'$ and $\mathbf{u} = [\delta_e, X_T, \delta_v, \delta_r]'$.

3 PATH-TRACKING PROBLEM

Let us start by define the vehicle mission: to force the output to follow a reference signal, a given function of time, and to drive to zero the tracking error:

$$\mathbf{e}(t) = \mathbf{y}(t) - \mathbf{y}_r(t) \qquad (8)$$

This *path-tracking problem* differs from the path-following one by the fact that the path reference is time dependent.

We define here the cartesian position error $\mathbf{e}_p = [\eta, \delta, \gamma]'$ as expressed in the reference path frame and computed by (see fig. 3)

$$\mathbf{e}_p = \mathbf{S}(\boldsymbol{\Phi}_r)(\mathbf{p} - \mathbf{p}_r) \qquad (9)$$

The reference path attitude $\boldsymbol{\Phi}_r = [\phi_r, \theta_r, \psi_r]'$ is obtained considering $\phi_r = 0$, and θ_r and ψ_r as the angles the reference trajectory does respectively with the horizontal plane, and the north direction.

The attitude error is the difference between the airship and reference attitudes:

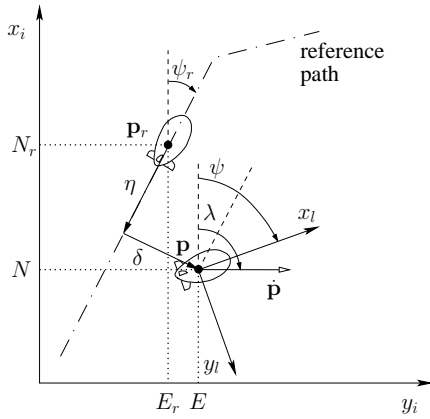$$\mathbf{e}_\Phi = \boldsymbol{\Phi} - \boldsymbol{\Phi}_{a_r} \qquad (10)$$

Figure 3: Position errors definition (2D).

If we were not taking into account the wind input, $\mathbf{\Phi}_{a_r} \equiv \mathbf{\Phi}_r$. However, due to the sideslip, the airship orients itself with the relative air direction (see fig. 4). Therefore, the attitude reference $\mathbf{\Phi}_{a_r}$ corresponds to the estimated attitude of the reference velocity influenced by the wind, $\hat{\dot{\mathbf{p}}}_{a_r}$.
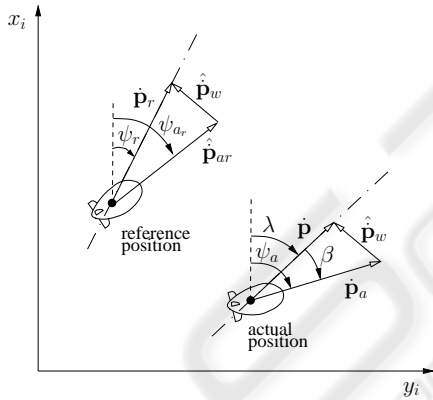

Figure 4: Reference heading estimation (2D).

We compute the reference attitude $\mathbf{\Phi}_{a_r}$ following these three steps:

1. with the airship inertial velocity $\dot{\mathbf{p}}$, its attitude $\mathbf{\Phi}$ and the aerodynamic variables V_t, β and α (all measured variables), estimate the wind inertial velocity vector $\hat{\dot{\mathbf{p}}}_w$ using equations (6) and (3), and knowing that $\dot{\mathbf{p}} = \mathbf{S}(\mathbf{\Phi})'\mathbf{v}$;

2. compute the velocity in the aerodynamic frame $\hat{\dot{\mathbf{p}}}_{a_r}$ as the inertial vectors difference between the airship reference velocity $\dot{\mathbf{p}}_r$ and the wind velocity estimation $\hat{\dot{\mathbf{p}}}_w$;

3. consider $\phi_{a_r} = 0$, and θ_{a_r} and ψ_{a_r} as the angles $\hat{\dot{\mathbf{p}}}_{a_r}$ does respectively with the horizontal plane,

and the north direction.

The objective of the control design proposed in the next section is then to drive to zero the errors given by equations (9) and (10).

4 GAIN-SCHEDULING

The linearized system model (7) presented before is only valid for small regions around trim conditions. This reveals the basic limitation of the design via the linearization approach, the fact that the controller is guaranteed to work only in the neighborhood of a single operating (equilibrium) point. The gain scheduling technique (Khalil, 2000b) addressed here allows to extend the validity of the linearization approach to a range of operating points, in this case over the entire flight envelope.

It is sometimes possible to find auxiliary variables that correlate well with the changes in the process dynamics. In the airship case, these variables mostly correspond to the airspeed V_t and altitude h. Still, the altitude influence may be disregarded for low altitude flights where the envelope pressure is kept practically constant. The airspeed, however, has a major influence over the airship behavior. It not only determines the magnitude of the aerodynamic forces acting on the airship, but also rules the influence of the actuators on the airship motion. As example, the action of the control surfaces, corresponding to the standard inputs δ_e and δ_r, is a function of the dynamic pressure and varies as the square of the airspeed (Stevens and Lewis, 1992), which leads to a reduced authority of these actuators when flying at low airspeeds.

Obtaining a linearized system at several equilibrium points, followed by the design of a linear feedback controller for each point, and implementation of the resulting family of linear controllers as a single controller whose parameters are changed by monitoring the scheduling variable, results in a gain scheduled controller (see figure 5). This controller is expected to maintain the stability and performance of the linear systems as long as the design models are reasonable representations of the system dynamics and as long as the scheduling variable varies "slowly".
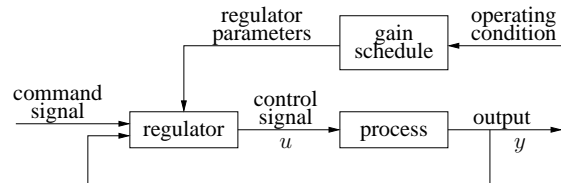

Figure 5: Gain-scheduling block diagram.

4.1 Optimal Control

Here we discuss the design of a servo control system whose purpose is to keep the tracking error small, while the airship flight condition is kept near the equilibrium state.

Consider the linear system defined by equation (7), assume the complete state $\mathbf{x}$ is measurable, and that the output variable

$$\mathbf{y} = \mathbf{Cx} \tag{11}$$

is to track a reference input $\mathbf{y}_r$. The tracking error is then defined as

$$\mathbf{e} = \mathbf{y} - \mathbf{y}_r \tag{12}$$

Considering that the model represents the deviations from an equilibrium state $\mathbf{X}_o$, it is required that the state variables $\mathbf{x}_c$ that do not form the output vector be kept null, in order to have $\mathbf{X}_c = \mathbf{X}_{c_o}$.

The admissible control is a proportional output feedback of the form

$$\mathbf{u} = \mathbf{K}_y\mathbf{e} - \mathbf{K}_c\mathbf{x}_c = -\mathbf{Kz} \tag{13}$$

where $\mathbf{z} = [\mathbf{e}', \mathbf{x}_c']'$ and $\mathbf{K} = [\mathbf{K}_y \ \mathbf{K}_c]$.

We use an optimal Linear Quadratic regulator to obtain the control effort (13), that results from the minimization of the cost function

$$J = \int_0^\infty (\mathbf{z}'\mathbf{Qz} + \mathbf{u}'\mathbf{Ru})dt \tag{14}$$

subject to the system dynamics (7). The state and control weighting matrices $\mathbf{Q} \geq 0$ and $\mathbf{R} > 0$ are the designer tools to balance the state errors $\mathbf{z}$ against the control effort $\mathbf{u}$. In the airship control case, the control weighting matrix $\mathbf{R}$ is a specially important tool in the sense that it allows the designer to change the control effort of the different actuators over the flight envelope.

The gain matrix $\mathbf{K}$ is obtained from

$$\mathbf{K} = \mathbf{R}^{-1}\mathbf{B}'\mathbf{P} \tag{15}$$

solving first the algebraic Riccati equation for the positive definite matrix $\mathbf{P}$

$$\mathbf{PA} + \mathbf{A}'\mathbf{P} - \mathbf{PBR}^{-1}\mathbf{B}'\mathbf{P} + \mathbf{Q} = 0 \tag{16}$$

The actuators request

$$\mathbf{U} = \mathbf{U}_o + \mathbf{u} \tag{17}$$

has to be computed for each linearized model, which means the procedure has to be repeated for different airspeeds. Figure 6 illustrates the closed-loop diagram for a determined equilibrium condition.
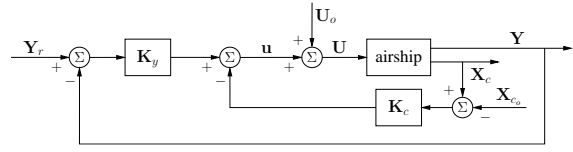

Figure 6: Linear control block diagram.

5 SIMULATION RESULTS

From the various simulations carried out, two examples are illustrated here concerning the same reference tracking: a nominal case with constant wind input and a case considering realistic wind disturbances, i.e., with an aleatoric component, which the airship platform is supposed to face during its normal operation.

In both cases the airship is to follow a reference path $\mathbf{p}_r(t)$ at constant altitude $h_r = -D_r = 50m$, starting deviated from the initial position at $\mathbf{p}_i = [-20, -10, -45]m$ and with the initial orientation $\mathbf{\Phi}_i = [10, 10, 10]deg$.

5.1 Nominal Case

This nominal case considers a constant wind input of $4m/s$ coming from north. The airship horizontal north-east trajectory with the correction from the initial deviation point and the cartesian position errors $\mathbf{e}_p = [\eta, \delta, \gamma]$ are shown in figure 7.
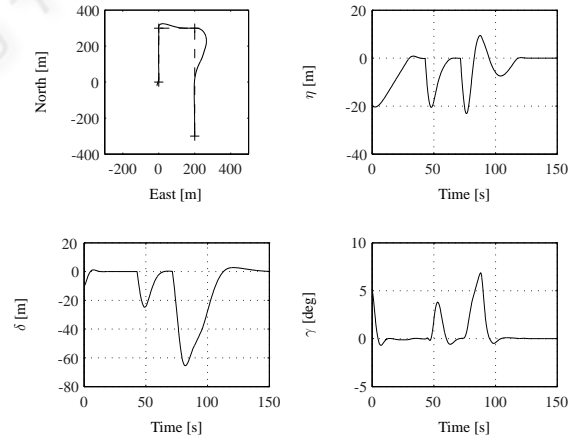

Figure 7: Nominal case: north-east trajectory (reference - dashed, output - solid), and position errors: longitudinal η, lateral δ and altitude γ.

After the initial deviation is corrected, the airship position errors stabilize to zero after passing the reference path corners.

So as to avoid saturation of the thrusters when the controller is correcting the airship position, the longi-

tudinal position error η was limited. This can be noticed by the constant rate at which the north position is corrected (η curve in fig. 7).

5.2 Realistic Case

In order to exemplify the controller robustness when in the presence of disturbances, further simulation tests included a 3D turbulent gust (simulated here by a Dryden model) with an intensity of $3m/s$ in addition to a constant wind blowing at $4m/s$ from north. The remaining setup values were the same used in the previous case.

Figure 8 shows the horizontal north-east trajectory and the cartesian position errors $\mathbf{e}_p = [\eta, \delta, \gamma]$. The airship behavior is similar to the nominal case, with the turbulent gust noticeable by the curves oscillation. Again, the position errors are corrected to zero, having the longitudinal error η been limited to avoid the thrusters saturation.
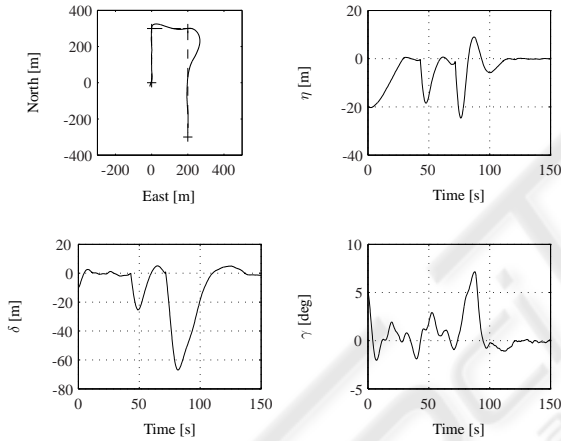

Figure 8: Realistic case: north-east trajectory (reference - dashed, output - solid), and position errors: longitudinal η, lateral δ and altitude γ.

The evolution of the airspeed V_t, represented in figure 9, defines the variations of the linear model used in the control design. The spam of the airspeed values over the flight envelope, between 2 and $12m/s$, is easily seen. This implies not only that the airship dynamics suffer a severe alteration, but also the actuators authority varies enormously. This can be confirmed comparing the airspeed curve with the graphics of the actuators input (elevator δ_e, total thrust X_T, vectoring angle δ_v and rudder δ_r) represented in figure 10.

Mostly we can observe the vectoring angle δ_v change between $0deg$ for aerodynamic flight, and $90deg$ at low airspeeds.

The sideslip angle β is also represented in figure 9. We can observe that its value oscillates around zero
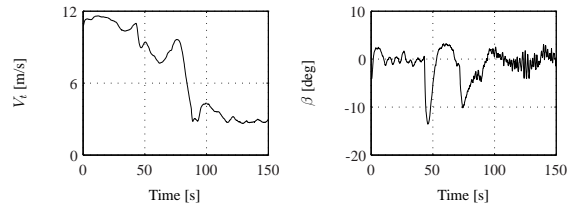

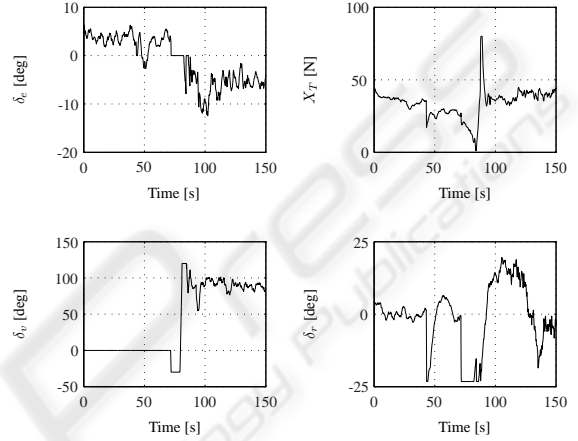Figure 9: Realistic case: airspeed V_t and sideslip angle β.

Figure 10: Realistic case: elevator δ_e, total thrust X_T, vectoring angle δ_v and rudder δ_r.

even though the airship is submitted to a wind disturbance. This achievement is due to the fact that the wind was included in the system model used to obtain the actuators request.

Finally we can observe in figure 11 that the rolling angle ϕ oscillates around zero, and the variation of the airship yaw ψ following the reference-path heading.
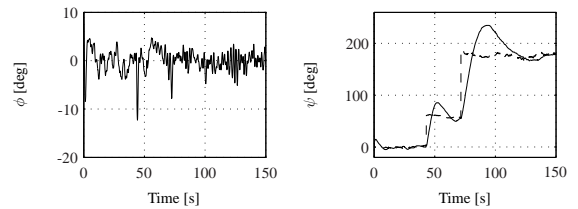

Figure 11: Realistic case: roll ϕ and yaw ψ angles (reference - dashed, output - solid).

As expected for low airspeeds, the control surfaces authority is reduced, which leads to a slower correction of the lateral errors in these situations.

6 CONCLUSION

In this paper a gain scheduled optimal controller is designed to solve the path-tracking problem of an airship, valid over the entire flight envelope. The control law is obtained from a coupled linear model of the airship that allows to control the longitudinal and lateral motions simultaneously. Due to the importance of taking into account wind effects, which are rather important due to the airship large volume, the wind is included in the kinematics, and the dynamics is expressed as function of the air velocity.

The examples presented with the inclusion of wind disturbances, demonstrate the effectiveness of this single controller tracking a reference path over the entire flight envelope. The implied variation of airspeed represents a significant problem in an airship control due to its influence to the system dynamics, as well as to the actuators authority.

REFERENCES

Åström, K. J. and Wittenmark, B. (1989). *Adaptive Control*, chapter 9: Gain Scheduling, pages 343–371. Addison-Wesley Publishing Company, 1st edition.

Azinheira, J. R., de Paiva, E. C., and Bueno, S. S. (2002). Influence of wind speed on airship dynamics. *Journal of Guidance, Control, and Dynamics*, 25(6):1116–1124.

de Paiva, E. C., Azinheira, J. R., Ramos, J. J. G., Moutinho, A., and Bueno, S. S. (2006). Project AURORA airship: Robotic infrastructure and flight control experiments. *Journal of Field Robotics*.

Elfes, A., Bueno, S. S., Bergerman, M., de Paiva, E. C., JR., J. G. R., and Azinheira, J. R. (2003). Robotic airships for exploration of planetary bodies with an atmosphere: Autonomy challenges. *Autonomous Robots*, (14):147–164.

Elfes, A., Bueno, S. S., Bergerman, M., and Ramos, J. J. G. (1998). A semi-autonomous robotic airshipfor environmental monitoring missions. In *Proceedings of the IEEE International Conference on Robotics and Automation*, volume 4, pages 3449–3455, Leuven, Belgium. IEEE Press.

Hygounenc, E. and Souères, P. (2003). Lateral path-following GPS-based control of a small-size unmanned blimp. In *Proceedings of the IEEE International Conference on Robotics and Automation*, volume 1, pages 540–545, Taipei, Taiwan. IEEE Press.

Khalil, H. K. (2000a). *Nonlinear Systems*, chapter 12: Feedback Control, pages 485–498. Prentice-Hall, Inc., 3rd edition.

Khalil, H. K. (2000b). *Nonlinear Systems*. Prentice-Hall, Inc., 3rd edition.

Merino, L., Caballero, F., de Dios, J. R. M., and Ollero, A. (2005). Cooperative fire detection using unmanned aerial vehicles. In *Proceedings of the IEEE International Conference on Robotics & Automation*, Barcelona, Spain.

Rao, J., Gong, Z., Luo, J., and Xie, S. (2005). Unmanned airships for emergency managment. In *Proceedings of the IEEE International Workshop on Safety, Security and Rescue Robotics*, pages 125–130, Kobe, Japan. IEEE Press.

Rugh, W. J. and Shamma, J. S. (2000). Research on gain scheduling - survey paper. *Automatica*, 36(10):1401–1425.

Silveira, G. F., Azinheira, J. R., Rives, P., and Bueno, S. S. (2003). Line following visual servoing for aerial robots combined with complementary sensors. In *Proceedings of the IEEE 11th International Conference on Advanced Robotics*, pages 1160–1165, Coimbra, Portugal. IEEE Press.

Stevens, B. L. and Lewis, F. L. (1992). *Aircraft Control and Simulation*. John Wiley and Sons, Inc., USA.

Xia, G. and Corbett, D. R. (2005). Cooperative control systems of searching targets using unmanned blimps. In *Proceedings of the 5th Worth Congress on Intelligent Control and Automation*, volume 2, pages 1179–1183, Hangzhou, P.R.China. IEEE Press.